COMPDYN 2015
5th ECCOMAS Thematic Conference on
Computational Methods in Structural Dynamics and Earthquake Engineering
M. Papadrakakis, V. Papadopoulos, V. Plevris (eds.)
Crete Island, Greece, 25–27 May 2015

UNCERTAINTY OF BRIDGE VIBRATION PROPERTIES AND ITS CONSEQUENCE FOR DAMAGE IDENTIFICATION

Marian Ralbovsky[1], Maciej Kwapisz[1], and Alois Vorwagner[1]

[1] AIT Austrian Institute of Technology GmbH
Giefinggasse 2, 1210 Vienna, Austria
e-mail: marian.ralbovsky@ait.ac.at
e-mail: maciej.kwapisz@ait.ac.at
e-mail: alois.vorwagner@ait.ac.at

Keywords: Uncertainty, Modal properties, Damage Detection, Clustering, Monte-Carlo Simulation.

Abstract. *This study deals with the topic of bridge health monitoring based on identification of bridge vibration properties, which are influenced by uncertainties. Focus is laid on quantification of the uncertainties from continuous monitoring data. The determined uncertainties are then used in probabilistic evaluation of structural state. The purpose is to acquire besides the "best-match" structural state also the reliability of identification. A method for automated extraction of modal parameters and evaluation of their uncertainties is presented. It comprises clustering and statistical evaluation of Stochastic Subspace Identification system poles. The statistical properties of modal parameters are used to build a set of probabilistic variables sampled using Monte-Carlo Simulation. The generated sets are used for probabilistic damage detection, which uses a forward approach of finding the best match within a database of precalculated structural states. The presented study was performed using monitoring data acquired on a prestressed concrete box-girder bridge in course of 9 months of continuous data recording.*

1 INTRODUCTION

Vibration-based damage detection on bridges is being applied since decades and it was the topic of research published in many articles and dissertations. The amount of published literature indicates that most researchers prefer data-only based approaches for damage detection. Maeck [1] described and applied in his dissertation different data-only detection algorithms, as well as some mixed approaches. Peeters [2] presented in his dissertation the advances in damage detection methods that are based on bridge modal properties (data-only), determined using Stochastic Subspace Identification (SSI) from continuous ambient vibration monitoring. The SSI-method represents a robust tool for system identification, which was later further improved [3]. The SSI-method was used also in this paper to extract bridge model properties. Santos [4] focused in his dissertation on novelty-detection and classification methods for damage detection purposes. Novelty detection aims to detect changed structural behavior from the measured data, and it represents level-1 damage identification. When combined with classification techniques [5] and a database of pre-calculated structural states, the measured structural parameters can be used for level-2 and level-3 identification. This approach was also applied in the work presented here. The model updating techniques aim at level-3 identification and solve the damage detection problem using an inverse approach that optimizes computational model [6]. The task of optimization of the bridge model puts high demands on computational effort. Therefore, the model should be small – built preferably using beam elements, particularly if the monitoring is continuous and the optimization must be performed repetitively.

The damage detection based on bridge vibration properties is affected by their accuracy and by the ability of post-processing techniques to compensate effects other than structural damages, which also influence vibration properties. Inaccurately determined vibration properties may cause that the wrong structural state will be matched with the measurements. The aim of the presented work was to evaluate accuracy of acquired vibration properties in one case study and to evaluate the effect that it had on selection of corresponding structural state (damage scenario). The presented approach uses the Monte-Carlo Simulation. Mares et.al. [7] used the approach of Monte-Carlo Simulation to investigate influence of modelling uncertainties on results of model updating (i.e. in the inverse problem). In the work presented here, the approach of Monte-Carlo Simulation is used in the forward problem.

The presented paper contains two technical chapters. Chapter 2 deals with uncertainty of modal parameters, and describes the sources of uncertainty and how the evaluation of uncertainties was implemented in an automated algorithm. Also, the measurement results and their statistical evaluation (uncertainty) are presented using data acquired on a prestressed concrete bridge in course of 9 months of continuous monitoring.

Chapter 3 intends to present the whole process of damage detection, starting with description of the tested bridge and installed monitoring system, further proceeding to creation of database of structural states, process of Monte-Carlo Simulation and results of probabilistic damage detection including simulated damage scenarios.

2 UNCERTAINTY OF MODAL PROPERTIES

The modal parameters of the bridge (eigenfrequencies, mode shapes, and damping ratios) are not only affected by structural damage, but vary also due to environmental influences and traffic intensity. Another source of uncertainty is the algorithm of modal parameter extraction. The process of dealing with measurement variations and uncertainties has two stages:

1. Compensation of known effects
2. Evaluation of remaining uncertainties

In the first stage, known effects can be compensated, if the relation between the influencing parameters and their effects is known. The purpose of the compensation is to reduce the magnitude of measurement variations. Typical example is the influence of temperature on bridge eigenfrequencies. Figure 1 shows the relation between measured eigenfrequencies and structural temperature acquired in presented case study.

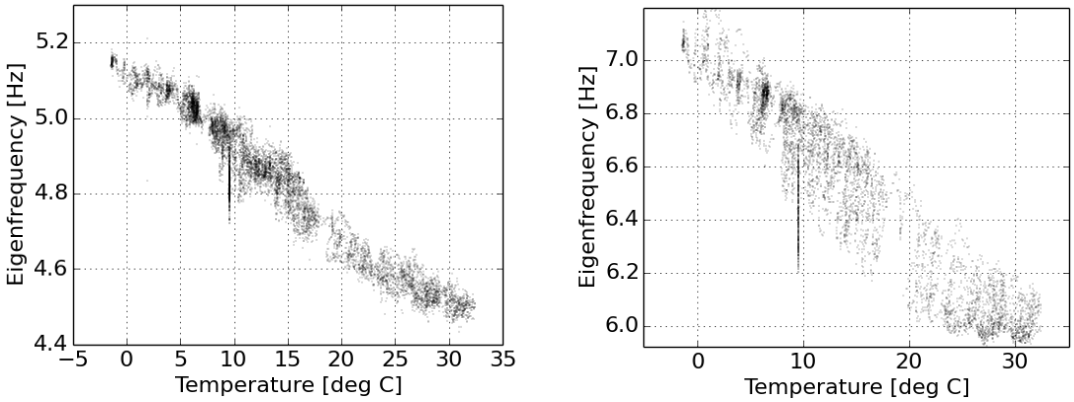

Figure 1: Relation between measured eigenfrequencies and structural temperature.

In the second stage, the remaining uncertainties are evaluated and form a basis for definition of input probabilistic variables for the Monte-Carlo Simulation. The evaluation of the uncertainties should be done using a scheme that can capture all expected sources of uncertainty that are still present in the compensated data. In the presented example, the expected sources of uncertainty after compensation of temperature effects were the following:

- Influence of traffic loads, including both changes of modal properties due to vehicle-bridge interaction, as well as due to the unknown excitation properties of dynamic axle forces. The extraction of modal parameters works well if the excitation source has properties of white noise. The actual excitation by traffic loads is not white noise, and it varies in time.
- Residual errors in temperature-compensation due to incomplete temperature information. The temperature is measured on few points in the structure and the distribution of temperature fields in the whole structure is not fully known.
- Other environmental influences, for example moisture and wind.
- Accuracy of the algorithm used for extraction of modal parameters, including both algorithm-inherent errors, as well as errors that originate from user interaction.

2.1 Automated extraction of system poles

To extract modal properties from measured accelerations, the Stochastic Subspace Identification (SSI) technique was used, which was well described by Peeters [2]. This chapter describes the procedure used for automated extraction of modal parameters and evaluation of short-term uncertainties. These include uncertainties related to traffic loads and to the extraction algorithm.

The variation of traffic loads was considered by application of overlapping time windows in the evaluation (Figure 2). As the traffic load varies in time, the dynamic excitation is dif-

ferent in each of the evaluated time windows. Data from each time window was processed by SSI separately. The identified system poles from 6 time windows were then grouped together and processed by clustering.

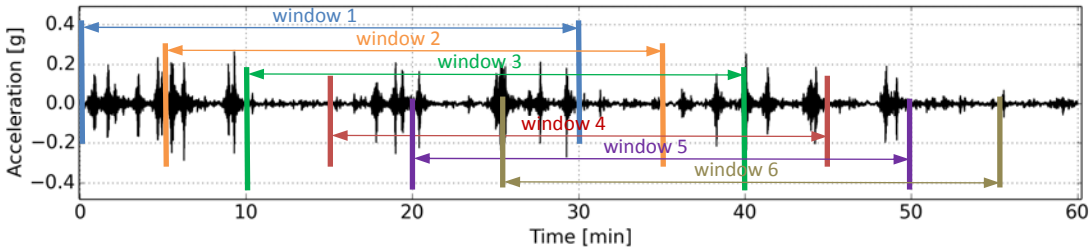

Figure 2: Overlapping time windows in data processing.

The SSI-method requires certain decisions to be made by the user. For example the user is expected to state the expected system order prior to the calculation and also to select the "correct" solution poles from among the many poles that were identified as possible solutions. The requirement of user interaction is not only impractical for processing of continuous monitoring data, but it is also the source of possible errors. Automated procedures that do not require user interaction were developed in the past for methods in frequency domain [8] as well as in time domain [3]. To evaluate the variation of solutions that could be selected from the SSI stabilization plot, the following procedure was applied. A relatively broad range of feasible model orders (Figure 3) was defined and all stable poles in this range were selected. Then, a clustering technique was applied to arrange the solutions into different groups. Each group of solutions contains stable poles of one mode. From each group, statistical moments of all variables could then be evaluated.

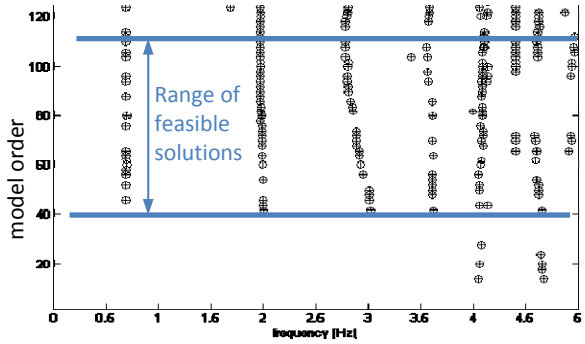

Figure 3: SSI stabilization plot showing identified stable poles.

2.2 Clustering of solutions

The purpose of clustering technique is to divide all feasible poles into groups, each representing one mode shape. A simple grouping of poles by range of frequencies is possible only in case of well separated modes. This was not the case at the given bridge, which has 8 spans with equal length, resulting in closely spaced modes. Therefore, a clustering technique had to be applied to sort the poles. The basis for application of clustering technique is calculation of a distance matrix, which defines the similarity between each pair of poles. The typical number of poles processed within one clustering run was around 1500, which resulted in a distance matrix with dimensions of 1500x1500. The distance between each pair of poles was calculated using similarity of frequencies (ratio f_i / f_j) and similarity of mode shapes (MAC value). The exact expression of distance between poles i and j is given in Equations 1 and 2.

$$D_{i,j} = 1 - MAC_{i,j} \cdot \left[r_{ij}\xi_j \left(\left(1 - r_{ij}^2\right)^2 + \left(2\xi_j r_{ij}\right)^2 \right)^{-0.5} + r_{ij}^{-1}\xi_i \left(\left(1 - r_{ij}^{-2}\right)^2 + \left(2\xi_i r_{ij}^{-1}\right)^2 \right)^{-0.5} \right] \quad (1)$$

$$r_{ij} = \frac{f_i}{f_j} \quad (2)$$

where f and ξ are identified frequency and damping ratio, respectively
$MAC_{i,j}$ is value of Modal Assurance Criterion
r_{ij} is the ratio of the frequencies.

The clustering algorithm groups together poles that have maximum distance between any two poles in the group smaller than a specified threshold. A small threshold produces many small groups, while a high threshold produces few large groups. This relation is displayed in Figure 4. The threshold needs to be specified by the analyst only once and is used for processing of all data from continuous monitoring. The threshold value used for the evaluation was in this case specified at 0.049.

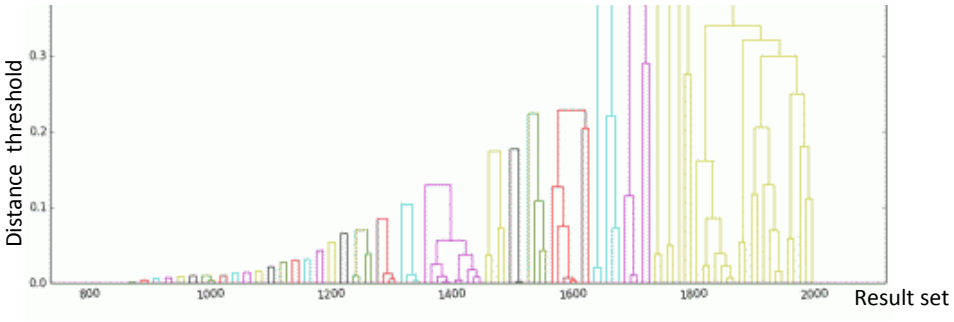

Figure 4: Clustering dendrogram.

The clustering algorithm tends to form large groups for poles with good stability. Therefore, small groups of poles can be sorted out as not relevant. In the presented case, any group containing less than 30 poles was not considered in following evaluations.

2.3 Statistical evaluation

Following the sorting of poles into groups by clustering, values in each group were statistically evaluated. The mean and the standard deviation were calculated for all modal parameters. Prior to this calculation, the modes were scaled to unity length and reversed if necessary to align the signs of mode shape values. As result, mean and standard deviation of frequency, damping, and all mode shape values were determined. Figure 5 shows the time history of one identified eigenfrequency. Displayed are the mean and the standard deviation, each evaluated using 1 hour of recorded data.

Figure 6 shows the variation of identified mode shape values in course of the whole monitoring period of 9 months. The presented histograms were calculated from mean mode shapes, whereas each mean mode was evaluated from one cluster, which contains identified poles using 1 hour of recorded vibration data.

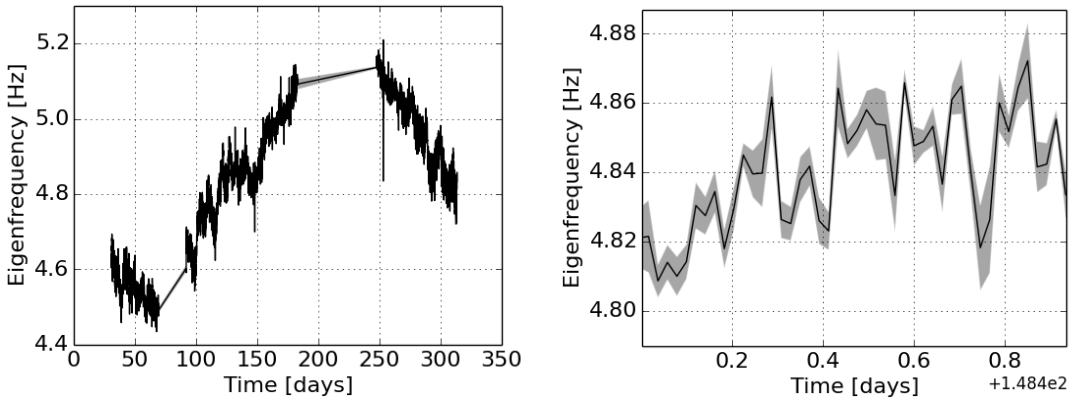

Figure 5: Eigenfrequency mean (black) and $\pm 1\sigma$ (grey) from all data (left) and in detail (right).

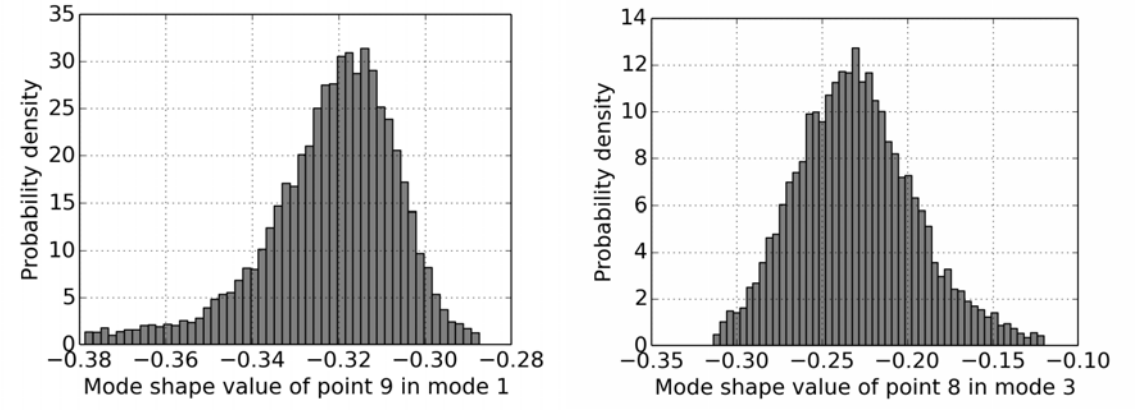

Figure 6: Two histograms that show variation of mode shape values, evaluated using data from 9 months.

The mode shape values at different measurement points show generally a good correlation. A strong correlation is advantageous for damage detection capability, since it narrows the space of random variations. Figure 7 shows the evaluated correlation matrix between mode shape values of all measurement points in two different mode shapes.

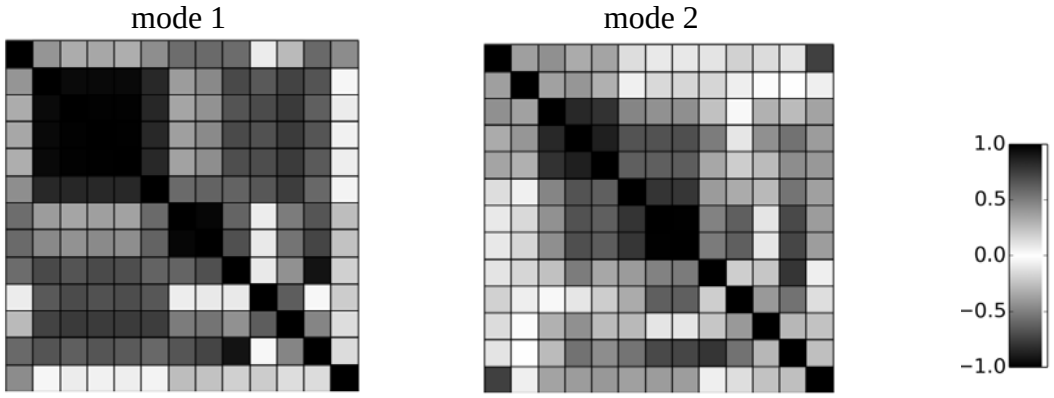

Figure 7: Matrix of correlation coefficients between mode shape values of all measurement points.

3 DAMAGE DETECTION

3.1 Test structure and monitoring system

The test structure is a prestressed concrete bridge with 10 spans. Its cross-section is a box-girder that is constant along whole length of the bridge. The cross-section has height of 3.2 m and the total length of the bridge is 327 m. Monitoring system was installed in the bridge, where different sensor types were used. For purposes of this study only data from the acceleration sensors were used. The position of the acceleration sensors is displayed in Figure 8. Sensors were placed in midspan of 9 spans, and few additional sensors at quarter-span positions were installed.

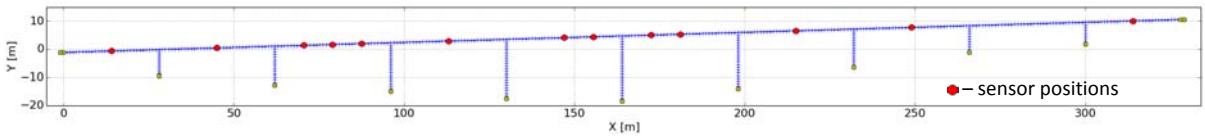

Figure 8: 2D-Finite Element model of the bridge and position of sensors

The acquired data used in this paper encompasses recordings from 9 months of data acquisition, containing both summer and winter periods.

3.2 Damage scenarios

Aim of this study was to investigate damage detection capability for the case of reduction of prestressing force in specific regions of the bridge. The reduction of prestressing force produces cracking in concrete and thus reduction of cross-sectional bending stiffness. A small reduction of prestressing force does not yet result in stiffness reduction because the whole cross-section is initially under compression. But after the tensile strength of concrete is reached and cracks occur, cross-sectional stiffness drops rapidly. Therefore, damage detection methods based on stiffness identification are most effective when detecting occurrence of first cracking.

A set of damage scenarios was calculated using the 2D Finite-Element model shown above. The damages scenarios were described by 3 parameters: position in the bridge, spatial extent (affected bridge length), and magnitude of bending stiffness reduction. Table 1 summarizes all damage scenario parameters.

Position	Affected bridge length [m]	Bending stiffness reduction [%]
Middle of span 1	2.8	2.2
Middle of span 2	4.7	11.5
Middle of span 3	8.5	20.8
Middle of span 4	10.4	30.1
Middle of span 5	12.3	39.3
Middle of span 6		48.3
Middle of span 7		57.3
Middle of span 8		66.3
Middle of span 9		…
Middle of span 10		86.6

Table 1: Properties of modeled damage scenarios.

There were 10 different damage positions, in each of them 5 different spatial extents (affected bridge length) were modeled, and in each of them 27 different stiffness reductions were modeled. This resulted in a total of 1350 damage scenarios that form a database. Modal parameters were calculated for each of the prepared damage scenarios. This database of model parameters in different damage scenarios serves for damage detection purposes. Using the measured modal parameters, one particular damage scenario can be found that shows the closest match with the measurements.

3.3 Monte-Carlo Simulation

Analysis of the forward propagation of measurement uncertainty was performed on the basis of Monte-Carlo Simulation. In the publication of Doebling [10], similar procedure to the approach used here is described. Doebling used definition of probabilistic input variables using normal distributions, and assumed that the variables are independent. Then, a set of input parameter samples was generated by application of appropriate sampling techniques. The work presented here uses similar approach. The main difference is that correlation of input variables was taken into account.

In chapter 2, the evaluation of uncertainty of measured modal parameters was described. The evaluated means, standard deviations and correlation coefficients were used to define a set of probabilistic variables. Each modal parameter (eigenfrequencies and mode shape values) was modeled as probabilistic variable with a normal distribution. The first two measured modes were used for damage detection. For each mode, 14 probabilistic variables were defined, which are the eigenfrequency and the mode shape values at 13 measurement points.

Matrix of correlation coefficients was defined according to results presented in chapter 2. In here, only the correlation coefficients of mode shape values within one mode have nonzero elements. The eigenfrequencies are considered as independent variables. Also, the correlation between values of two different modes was assumed to be zero.

The Latin Hypercube Sampling technique was used for generation of the sample set, which had the size of 1000 samples for each variable. Figure 9 shows an example of values generated by Latin Hypercube Sampling for two probabilistic variables with strong correlation. Displayed are values of mode shape 2 at point 4 vs. at point 3, which have a correlation coefficient of 0.86.

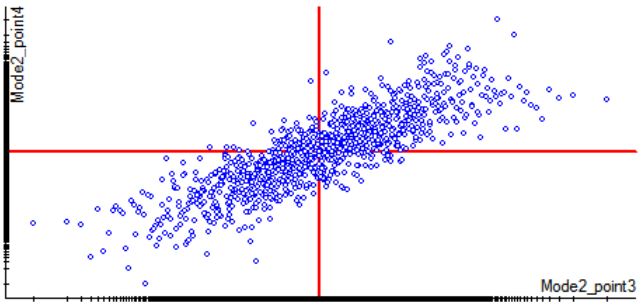

Figure 9: Generated samples of two mode shape values with strong correlation.

3.4 Probabilistic damage detection

To investigate the influence of modal parameter uncertainties on damage detection results, damage detection was performed for each sample of modal parameters generated by Latin Hypercube Sampling. In here, all generated samples represent healthy structural state. Ideally, the damage detection would result in 100% of the generated samples assigned to healthy structural state.

The damage detection for each sample of modal properties was done by comparing it to the database of pre-calculated damage scenarios. The damage scenario that matches best the sample of modal properties is selected as the identified damage case. Measure of match similarity was calculated according to Equation 3. In here, the frequency differences are normalized by standard deviation of measured frequencies and summed up. Then, measure of similarity of mode shapes is added, again normalized by standard deviation of MAC-values.

$$J_{i,d} = \sum_m \frac{\left| f_{i,m} - f_{d,m} \right|}{\sigma\left(f_m\right)} + \sum_m \frac{1 - MAC\left(\phi_{i,m}, \phi_{d,m}\right)}{\sigma\left(MAC\left(\phi_m\right)\right)} \tag{3}$$

where $J_{i,d}$ is objective function for matching modal parameter set i with damage scenario d,

$f_{i,m}$ is eigenfrequency of modal parameter set i of mode m,

$f_{d,m}$ is eigenfrequency of mode m in damage scenario d,

$\sigma(f_m)$ is standard deviation of eigenfrequency of mode m,

$MAC(\phi_{i,m}, \phi_{d,m})$ is Modal Assurance Criteria between modal parameter set i and damage scenario d of mode m,

$\sigma(MAC(\phi_m))$ is standard deviation of MAC-value between generated modal parameter sets and mean mode shape of mode m.

The standard deviation of MAC-values was evaluated by calculating MAC-values between all generated mode shapes and the mean mode shape. Histogram of these MAC-values is shown in Figure 10 for two modes. Table 2 lists standard deviations of frequency and MAC-value for the first two measured modes.

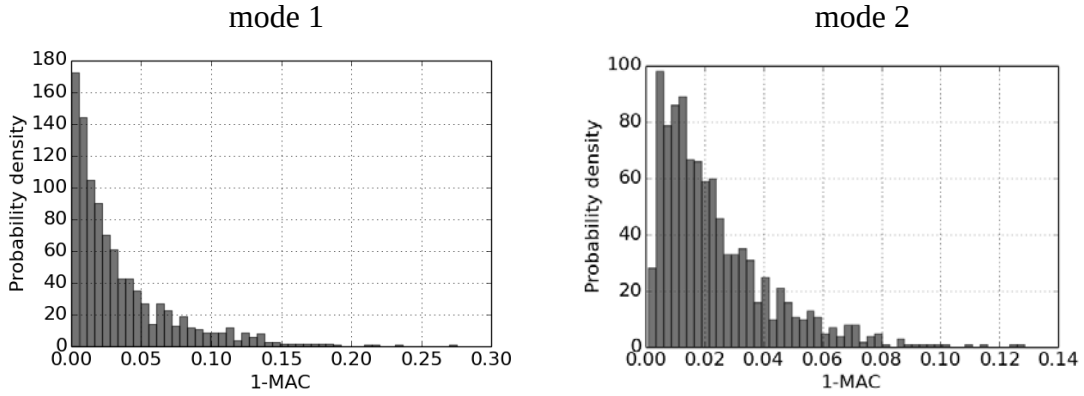

Figure 10: Histogram of MAC-values between generated mode-shape sets and the mean mode shape.

Mode	σ (f) [Hz]	σ(1-MAC) [-]
1	0.025	0.038
2	0.032	0.019

Table 2: Standard deviations of measured frequencies and MAC-values.

For each generated set of modal parameters i, the objective function $J_{i,d}$ is evaluated for all damage scenarios d. Then, the damage scenario with lowest objective function is picked. The procedure is repeated for all generated sets and thus a set of matching damage scenarios is acquired. The last step in this probabilistic damage detection is evaluation of occurrence frequency of particular damage scenarios. Results of this evaluation of occurrence frequency are visualized in the following figures.

The visualization contains quite complex information that has to be displayed together in one picture. Therefore, the following visualization rules were adopted:

- Each of the displayed vertical bars shows 4 properties: position of damage, spatial extent of damage, stiffness reduction E_{red}, and the probability that the stiffness reduction (E_k) is larger than E_{red}.
- The position and spatial extent of damage is displayed by position and width of the vertical bars on the axis called “Bridge coordinate”.
- The stiffness reduction E_{red} is displayed using the color code.
- The height of the bar defines the probability that the stiffness reduction is larger than E_{red} at the given position and spatial extent of the damage scenario.
- Vertical position of the blue rectangle defines the probability of healthy structural state (no damage)

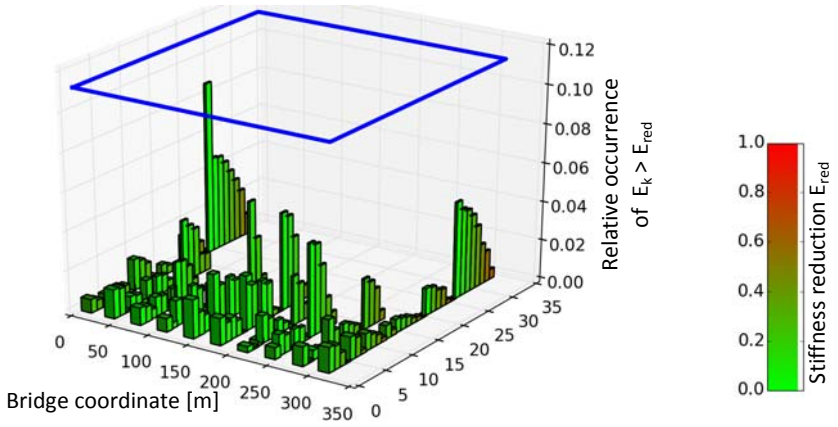

Figure 11: Relative occurrence of matching damage scenarios in healthy structural state.

From the figure above it can be seen that the healthy structural state (blue rectangle) has higher probability than any other damage scenario, therefore the structure is most likely undamaged.

In this type of visualization, the bars that would indicate high probability of damage would be red and high. On the other hand, a high green bar would represent a high probability of small stiffness reduction. Additionally, width of the bar indicates how localized the damage is.

Further, in this type of visualization it can be seen how good the localization of the damage is. In the figure above, different damage scenarios have small probabilities of occurrence. However, these damage scenarios are spread across the whole bridge length and do not concentrate on one region. This fact reinforces the conclusion that the structure is in healthy state.

In order to demonstrate results of probabilistic damage detection at occurrence of damage, the measured modal parameters were modified using simulated damage scenarios and the probabilistic damage detection was repeated. Figure 12 shows results of damage identification for simulated damage of stiffness reduction at bridge coordinate X=113.8m, affected bridge length was L=4.7m and magnitude of stiffness reduction was E_k=11.5% and E_k=30%, respectively. The displayed results show that the blue rectangle has a low position, which means the structure is not likely in healthy state. The matching damage scenarios concentrate more in one region, which indicates the likely position of damage. It can be observed that certain wide green bars have similar height as other narrow orange bars, which means that the probability of small stiffness reduction on a larger area is approximately equal to probability of higher stiffness reduction on a more localized area.

Simulated damage: X=113.8m, L=4.7m, E_k=11.5 % X=113.8m, L=4.7m, E_k=30 %

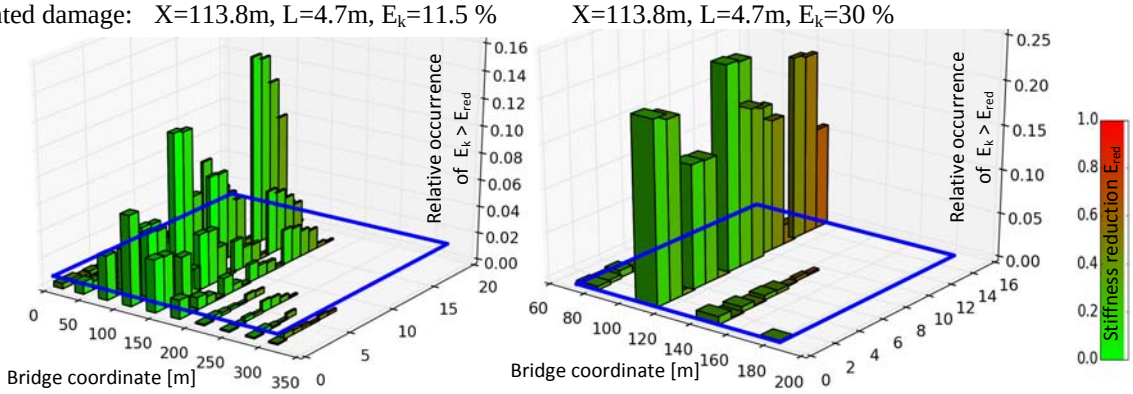

Figure 12: Relative occurrence of matching damage scenarios in two simulated damage cases.

Figure 13 shows a similar evaluation for a different position of simulated damage (X=181.5m) and larger affected bridge length (L=12.3m). In both simulated damage scenarios, the damage can be quite well localized at a stiffness reduction of 30%.

Simulated damage: X=181.5m, L=12.3m, E_k=11.5 % X=181.5m, L=12.3m, E_k=30 %

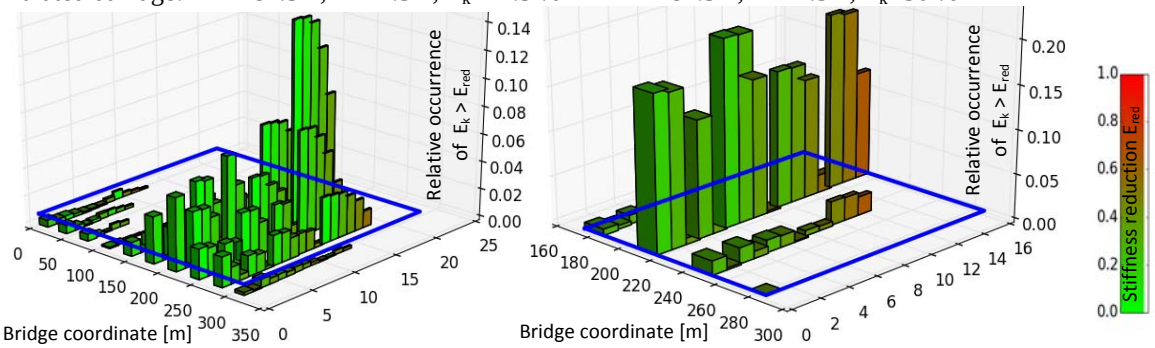

Figure 13: Relative occurrence of matching damage scenarios in other two simulated damage cases.

Figure 14 shows results for a simulated damage with a high stiffness reduction (E_k=57.3 %). The high probability of identified damage is indicated by presence of high red bars. The damage localization is unambiguous.

Simulated damage: X=113.8m, L=4.7m, E_k=57.3 %

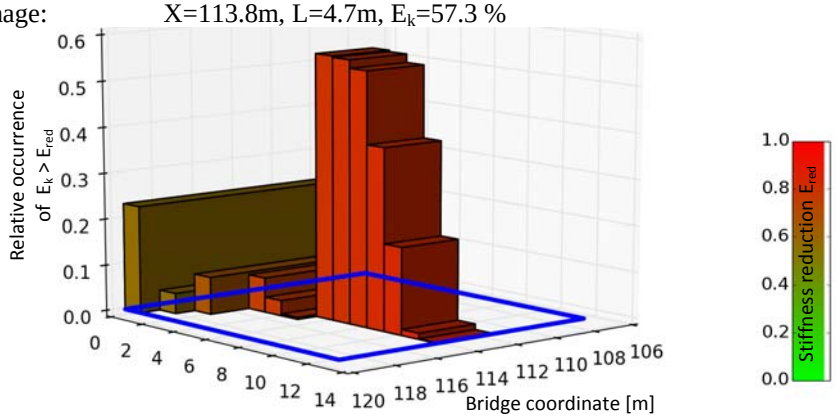

Figure 14: Relative occurrence of matching damage scenarios in a simulated damage case with high stiffness reduction.

4 CONCLUSIONS

- Procedure for evaluation of modal parameter uncertainties was presented. It is recommended to consider besides uncertainties caused by environmental influences also the uncertainties of the automated extraction of modal parameters.
- Damage detection was performed using the forward approach by matching of modal parameters to database of pre-calculated damage states.
- Effect of modal parameter uncertainty on damage detection results was evaluated using Monte-Carlo Simulation.
- Healthy structural state was clearly identified by relatively high probability of undamaged state and smaller probabilities of weak damage scenarios spread across the whole bridge (not localized in any specific area).
- In the simulated damage scenarios, the localization became clearer if the introduced stiffness reduction was higher. Already at level of 30 % stiffness reduction the localization was very good.
- The presented probabilistic process of damage detection seems to be a practicable method for damage detection that considers uncertainties of input parameters.

ACKNOWLEDGEMENTS

Part of the presented work was accomplished within the research project TRIMM (Tomorrow's Road Infrastructure Monitoring and Management), which was part of FP7 research programme funded by the European Commission.

REFERENCES

[1] J. Maeck, *Damage Assessment of Civil Engineering Structures by Vibration Monitoring*, PhD thesis, Katholieke Universiteit Leuven, 2003.

[2] B. Peeters, *System identification and Damage Detection in Civil Engineering*, PhD thesis, Katholieke Universiteit Leuven, 2000.

[3] J. Lau, J. Lanslots, B. Peeters, H. Van der Auweraer, *Automatic modal analysis: reality or myth?*, 25th International Modal Analysis Conference, Orlando, USA, February 2007.

[4] J. P. Santos, *Smart Structural Health Monitoring Techniques for Novelty Identification in Civil Engineering Structures*, PhD thesis, Universidade de Lisboa, Instituto Superior technico, 2014.

[5] Ch. Efstathiades, C.C. Baniotopoulos, P. Nazarko, L. Ziemianski, G.E. Stavroulakis, *Application of neural networks for the structural health monitoring in curtain-wall systems*, Engineering Structures vol. 29, pp.3475–3484, 2007.

[6] J.M.W. Brownjohn, P.-Q. Xia, H. Hao, Y. Xia, *Civil structure condition assessment by FE model updating: Methodology and case studies*. Finite Elements in Analysis and Design vol. 37, pp. 761-775, 2001.

[7] C. Mares, J.E. Mottershead, M.I. Friswell, *Stochastic model updating: Part 1- theory and simulated example*, Mechanical Systems and Signal Processing vol. 20, pp. 1674–1695, 2006.

[8] P. Verboven, E. Parloo, P. Guillaume, M. Van Overmeire, *Autonomous Structural Health Monitoring – Part 1: Modal Parameter Estimation and Tracking*, Mechanical Systems and Signal Processing vol. 16, pp. 637–657, 2002.

[9] M. Döhler, L. Mevel, P. Andersen, *Efficient uncertainty computation for modal parameters in stochastic subspace identification*. 4th International Conference on Uncertainty in Structural Dynamics, Leuven, Belgium, 2012.

[10] S. W. Doebling, F. M. Hemez, *Overview of Uncertainty Assessment for Structural Health Monitoring*, 3rd International Workshop on Structural Health Monitoring, Stanford, USA, September 2001.